Geochronologic and Pb-isotopic constraints on gold mineralization at the Plateau South property (Yukon MINFILE 105N 034, 035, 036), central Yukon

P. Sack*
Yukon Geological Survey

J. Gabites
University of British Columbia

J. Crowley
Boise State University

J. Benowitz
University of Alaska Fairbanks

C. McFarlane
University of New Brunswick

M. Gobadi
Activation Laboratories Ltd.

D. Ferraro
Goldstrike Resources Ltd.

Sack, P., Gabites, J., Crowley, J., Benowitz, J., McFarlane, C., Gobadi, M. and Ferraro, D., 2020. Geochronologic and Pb-isotopic constraints on gold mineralization at the Plateau South property (Yukon MINFILE 105N 034, 035, 036), central Yukon. *In:* Yukon Exploration and Geology 2019, K.E. MacFarlane (ed.), Yukon Geological Survey, p. 99–119.

Abstract

Quantitative mineralogy, U-Pb geochronology of zircon and monazite, $^{40}Ar/^{39}Ar$ geochronology of muscovite and sericite, and Pb isotopes from galena in veins and feldspar in plutons provide insight into the age of metamorphism, mineralization, intrusion emplacement and the sources of metals at the Plateau South (MINFILE 105N 034, 035, 036) occurrences in central Yukon. Orogenic mineralization and metamorphism is *ca.* 110 Ma to 100 Ma, and possibly as old as *ca.* 130 Ma. Following deformation and regional metamorphism, two biotite-muscovite plutons, the Russell stock and Armstrong pluton, were emplaced at 95.39 ± 0.03 Ma and 95.51 ± 0.03 Ma, respectively. These plutons are here reassigned to the Tungsten suite based on mineralogy, chemistry and age. Coeval with these plutons are contact metamorphism and possibly intrusion-related mineralization. Lead isotopic data from galena cluster into two groups: Group 1 is enriched in thorogenic Pb with $^{206}Pb/^{204}Pb$ values between 18.31 and 18.14, $^{207}Pb/^{204}Pb$ between 15.62 and 15.55 and $^{208}Pb/^{204}Pb$ between 38.77 and 38.30. Group 2 is isotopically evolved with $^{206}Pb/^{204}Pb$ values between 19.13 nd 18.91, $^{207}Pb/^{204}Pb$ between 15.78 and 15.63 and $^{208}Pb/^{204}Pb$ between 39.24 and 39.07. We suggest that late Early Cretaceous mineralization is related to large-scale orogenic fluids that tapped primitive (deep?) metal sources and early Late Cretaceous mineralization, coeval with local intrusions, sourced isotopically distinct metals from the intrusions. Alternatively, all mineralization could relate to Early Cretaceous orogenic fluids but with heterogeneous, locally derived metal sources and thermal resetting of Ar ages near the intrusions.

* patrick.sack@gov.yk.ca

Introduction

The Plateau South property was initially staked in 2011 and since then more than 20 breccia and vein gold showings have been found across a 50 km area; the veins and property geology are described in more detail in Sack et *al.* (2018). The Plateau South showings often contain visible gold and are reminiscent of orogenic gold veins though previous work points out that mineralization also shares similarities with reduced-intrusion related gold deposits (Sack et *al.*, 2018) which are well known in the Selwyn basin area (e.g., Hart et *al.*, 2004). To help discriminate between an orogenic and intrusion-related origin for the veins in the Plateau area, a suite of samples was collected in 2016 and 2017 for geochronology and Pb isotopic analyses. Here, we present and discuss these data and use them to constrain the age of metamorphism, mineralization, intrusion emplacement and the sources of metals in the veins at the Plateau property in central Yukon.

Geology

The Plateau property lies within basinal ancestral North America rocks of the northern Canadian Cordillera (Fig. 1). The property is mostly underlain by Neoproterozoic to Cambrian rocks of the Hyland Group, mostly the Yusezyu Formation (Fig. 2). The Yusezyu Formation rocks are coarse to fine-grained sandstone and siltstone with pebble conglomerate interbeds that have been regionally metamorphosed to greenschist facies and are now phyllite to schist (Sack et *al.*, 2018).

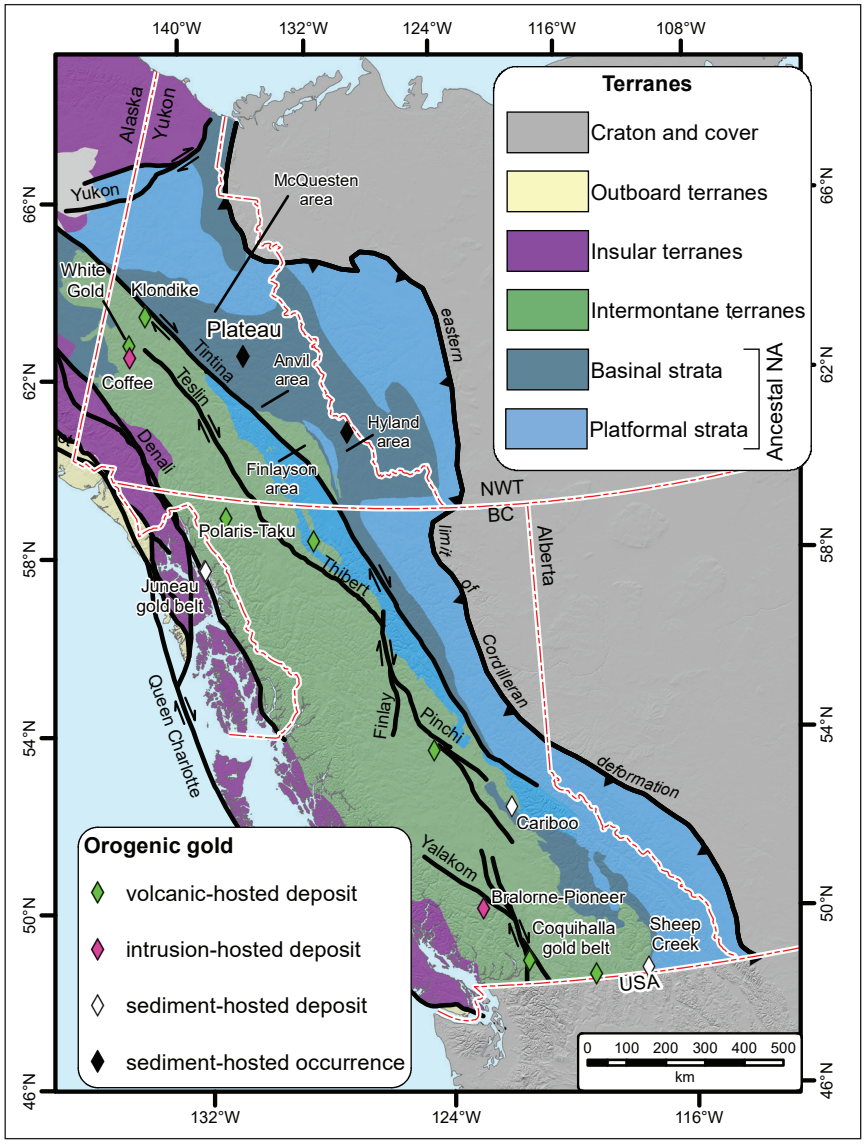

Figure 1. *Terranes, regional faults, significant orogenic gold deposits and camps of British Columbia and Yukon. Deposits from Goldfarb et al. (2005), Dubé and Gosselin (2007) and YGS (2018a). Terranes from Colpron and Nelson (2011). NA = North America. Note location of Hyland, Anvil, McQuesten and Finlayson areas used to frame regional geochronology discussion.*

At the property scale, the Yusezyu Formation is subdivided into units that are dominantly psammite and pelite (Roach, 2013; Stubley, 2017; Vanwermeskerken, 2017) with all of the known veins hosted in the psammite unit. A thin, concordant body of chloritic phyllite in the Big Bang zone (Fig. 2) is interpreted as a mafic volcanic rock or sill (Stubley, 2017), possibly correlating with the Old Cabin Formation of Cecile (2000); mafic rocks are also found 30 km to the south (Roots, 2003). Paleozoic shale of the Gull Lake, Road River and Earn groups, as well as the Mt Christie, Tsichu and No Gold formations (Roots, 2003) is found to the northeast and southwest of the area. The Yusezyu Formation is intruded by the Russell stock and Armstrong pluton. These plutons are medium-grained, equigranular, and biotite-muscovite ± hornblende ± garnet bearing granite to granodiorite intrusions having low magnetic susceptibility (<0.1 × 10^{-3} SI units; Sack et *al*., 2018).

The Plateau property mostly lies within the Tombstone strain zone (Murphy, 1997), the southern (upper) boundary of which is approximated by the thick dashed line on Fig. 2 (Roots et *al*., 1995; Roots, 1998). This boundary broadly subdivides the property into two structural domains and is coincident with many of the vein showings (Sack et *al*., 2018). The southern domain has upright folds with steep axial planar cleavage and the northern domain comprises inclined to recumbent folds with low-angle axial planar cleavage (Stubley, 2017). The upright domain structurally overlies the shallow domain. Though the detailed structural history varies slightly between the domains, they each have a well developed early axial planar cleavage developed around broadly NW or SE fold axes and a later, less intense crenulation cleavage (Sack et *al*., 2018). Mineralized breccia in the Goldstack zone forms an elongate body, as defined by limited diamond drilling,

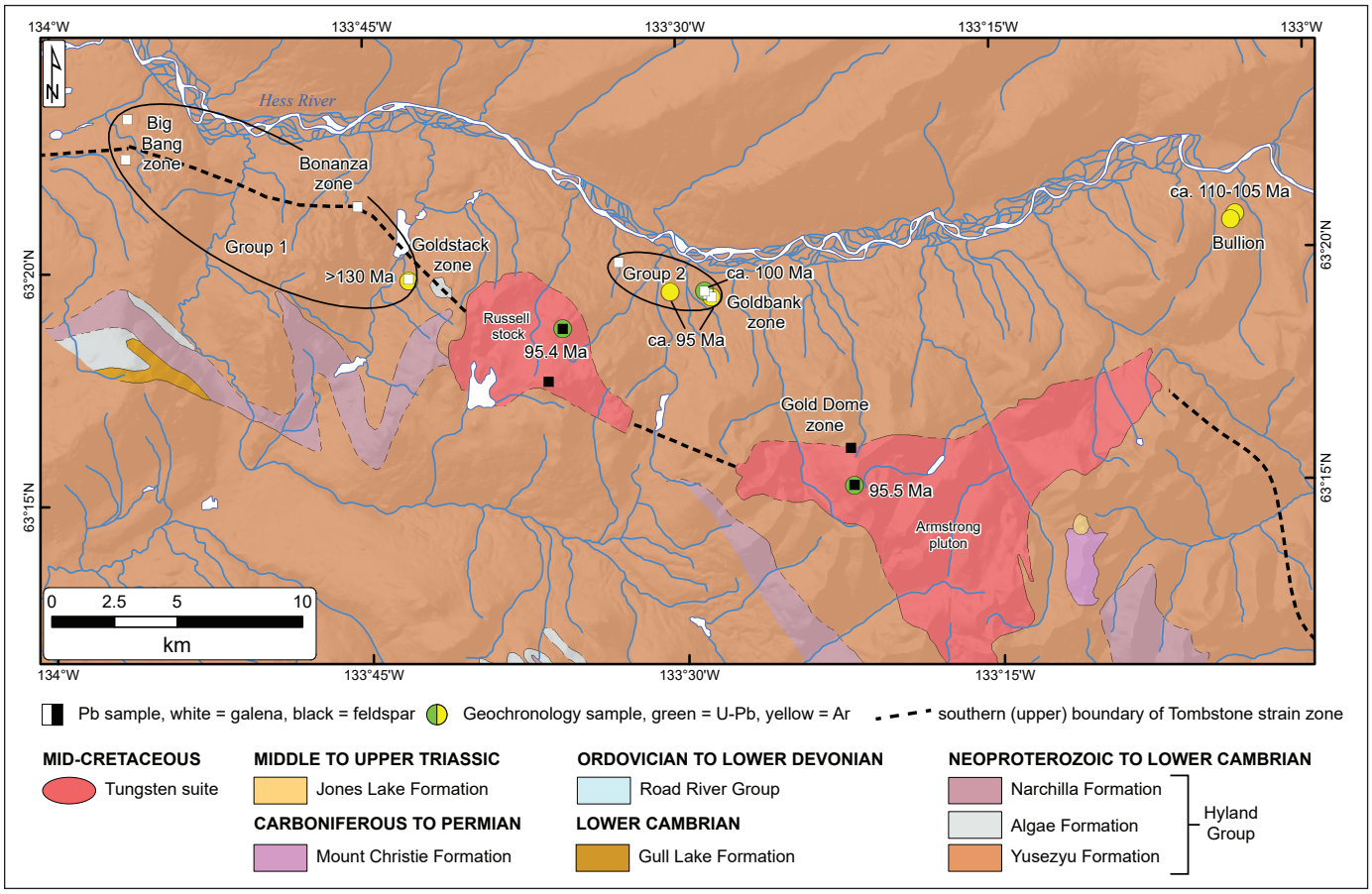

Figure 2. *Simplified Plateau property geology from YGS (2018b). Geochronology labels are those cited in text and Table 1. Groups 1 and 2 are based on Pb isotopic data from Table 3. For more information on the detailed geology, showings and claim boundaries in this area see Fig. 4 of Sack et al. (2018).*

that strikes NW, and appears to be in the antiformal hinge of a fold in the upright domain; the orientation of other breccia showings is not known. Mineralized veins are dominantly NE striking extensional veins that crosscut all earlier structures and fabrics but are variably deformed and recrystallized suggesting formation late in the ductile deformation history (Sack et *al*., 2018). Plutons in the area are undeformed and have contact aureoles that overprint foliation, thus indicating emplacement after ductile deformation (Fig. 3; Sack et *al*., 2018).

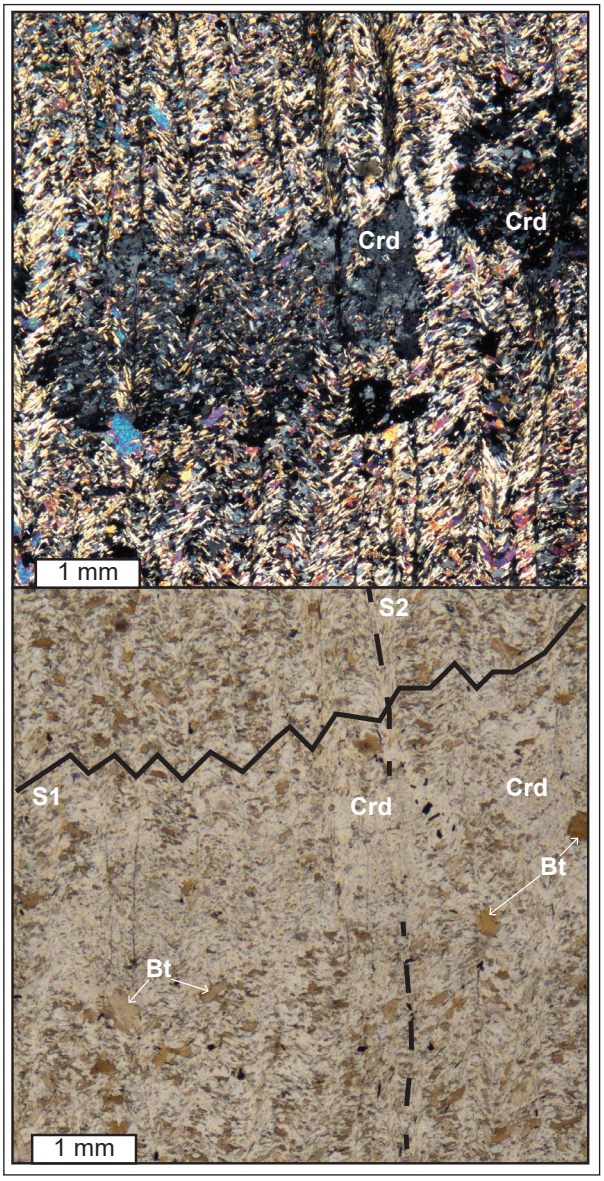

Figure 3. *Cross-polarized* ***(upper)*** *and plain polarized* ***(lower)*** *photomicrographs of cordierite overgrowing two generations of foliation in pelite (17PS009-1) (Sack et al., 2018). Birefringent mineral is muscovite. Crd = cordierite, Bt = biotite.*

Mineralization on the Plateau South property can be broadly divided into breccia bodies that may strike NW and massive, discrete, white quartz veins that strike NE. The Goldstack, Big Bang zones and possibly Gold Dome have breccia style showings but most of the showings are individual, or sets of, discrete NE striking veins (Sack et *al*., 2018). In both styles of mineralization, the earliest quartz is massive and recrystallized, commonly with reduced grain boundaries and strong undulatory extinction (Fig. 4a). Associated coarse-grained euhedral arsenopyrite is typically fractured (Fig. 4b). Later quartz-sulphide ± muscovite ± carbonate ± plagioclase (albite?) veins crosscut earlier veins. Gold is associated predominantly with arsenopyrite (Fig. 4c) but also with pyrite and pyrrhotite. Minor galena and chalcopyrite are noted locally (Richards, 2015).

Despite the different orientation and appearance, the similar mineralogy and paragenesis has lead previous workers to infer a shared origin for vein and breccia type showings (Barr, 2017; Farquharson, 2017; Sack et *al*., 2018). Galena in the vein showings occurs as anhedral fracture-fill in arsenopyrite or as anhedral masses within the veins (Fig. 6) and is interpreted as a pargenetically late mineral. Where galena fits in the paragenesis of the breccia showings is not constrained in thin section. Correlation coefficient (r^2) values between Au and Ag, As, Pb and Sb for all showings range between 0.6 and 0.1, consistent with the presence of arsenopyrite in all gold bearing veins and galena in some (Sack et *al*., 2018).

Methods

We use five data sets in this paper: (1) whole-rock geochemistry; (2) quantitative mineralogy; (3) U-Pb zircon geochronology for plutons and U-Pb monazite for psammitic schist; (4) Ar geochronology of muscovite from psammitic schist and sericite from veins; and (5) Pb isotopes from galena in veins and feldspar in plutons. A brief method summary for each data set is given below; further details for each method are in the appendices or in cited references.

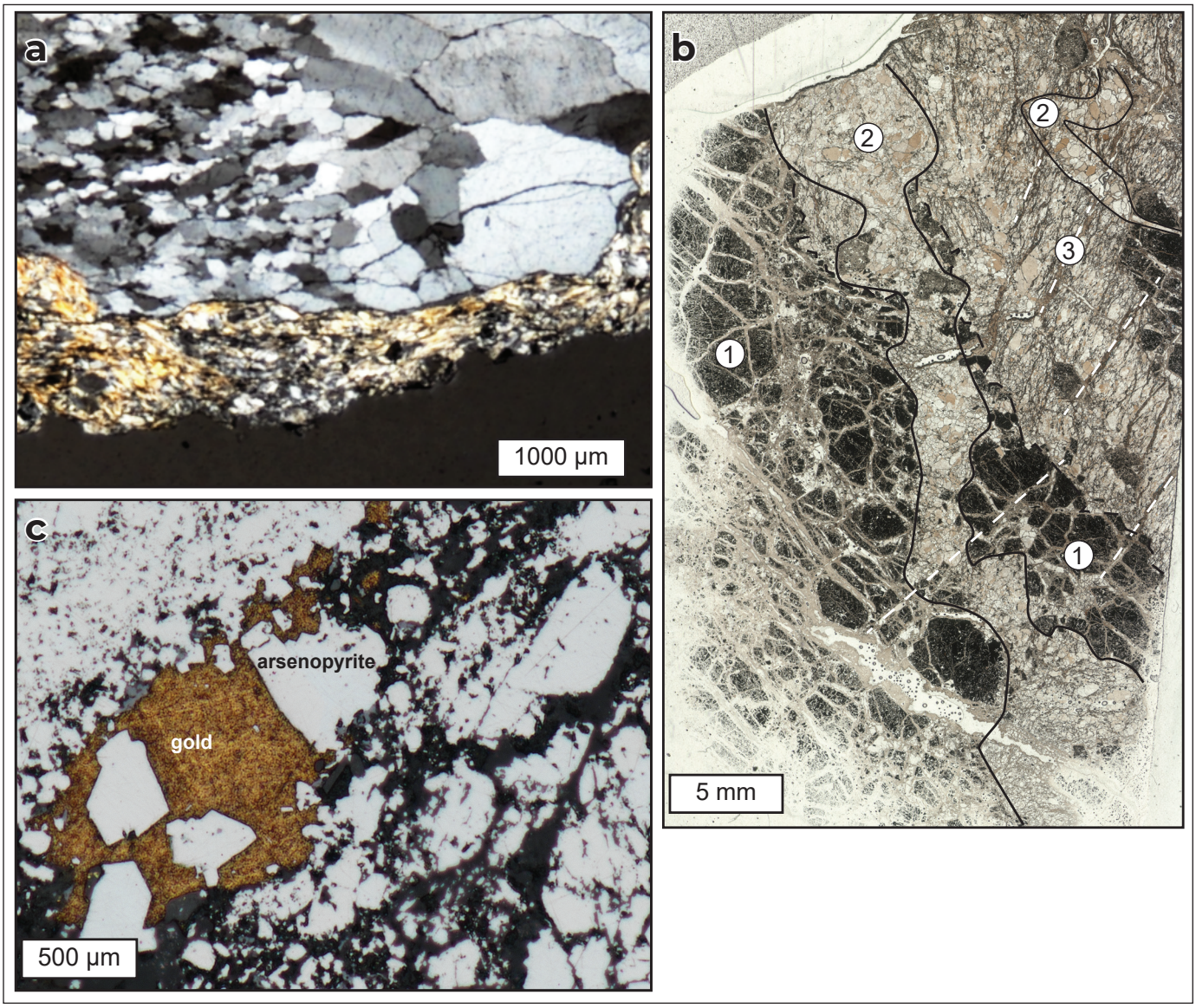

Figure 4. *Mineralized veins on the Plateau South property.* ***(a)*** *Breccia style with early recrystallized quartz cut by later, thin quartz-sericite-carbonate veinlet, Bonanza zone, 16PS001-1 (Sack et al., 2018).* ***(b)*** *Plane polarized light thin section scan illustrating paragenesis for vein style mineralization at the Ron Stack vein, Goldbank zone (17PS028-2): 1 – early brittle deformed arsenopyrite vein; 2 – folded and variably recrystallized quartz veins that cut 1; and 3 – foliation that penetrates 1 and 2.* ***(c)*** *Native gold intergrown with arsenopyrite PSGS1502-37.60m, Goldstack zone.*

Whole-rock geochemistry

Whole-rock analysis of four pluton and five country rock samples was conducted at Activation Laboratories Ltd. The analytical package was 4Lithoresearch, a lithium metaborate/tetraborate fusion followed by Inductively Coupled Plasma Mass Spectrometry (ICPMS). For major elements, the quality of these data meet or exceeds fusion x-ray fluorescence data. For trace elements, the fusion process provides total dissolution of refractory minerals such as zircon, sphene and monazite, and gives accurate rare earth and high field strength element data. Precision for major elements is typically <5%; trace and rare earth element precision is typically <10%. Major and rare earth element accuracy is <10%; trace element accuracy is <20%. Data are in Appendix 1.

Mineralogy

Quantitative mineralogy and mineralogical mapping using QEMSCAN (quantitative evaluation of materials by scanning electron microscopy) were conducted at Activation Laboratories on three parallel cut thin sections from one breccia style showing and one vein style showing. Data are in Appendix 1

U-Pb geochronology

Two plutonic samples underwent U-Pb zircon geochronological analysis at Boise State University. Data include cathodoluminescence (CL) images of zircon, and results of laser ablation-inductively coupled plasma mass spectrometry (LA-ICPMS) and chemical abrasion-thermal ionization mass spectrometry (CA-TIMS). We use the more precise weighted mean date of CA-TIMS analyses to determine the crystallization age of each sample. Errors are reported at 2σ. Data are in Appendix 2

U-Th-Pb monazite geochronology for one wall rock sample was carried out at the University of New Brunswick. Monazite grains were located using QEMSCAN and were imaged with a scanning electron microscope in backscatter emission mode (SEM-BSE). U-Th-Pb data were collected using LA-ICPMS with a laser crater diameter of 13 µm, a laser pulse rate of 3 Hz, 3 J/cm^2 laser fluence, and 30 seconds of ablation after 30 seconds of gas background collection. Errors are reported at 2σ. Data are in Appendix 2

Ar geochronology

Argon geochronology for five samples was completed at the Geochronology Laboratory at the University of Alaska Fairbanks; two muscovite samples from country rock and three sericite samples from mineralized rocks. Samples were crushed, sieved, washed and hand-picked for pure muscovite and sericite separates. Samples were irradiated and subsequently analyzed for $^{40}Ar/^{39}Ar$ using step-heating and mass spectrometry. Analysis for each sample consists of eight steps and ages are primarily interpreted from plateau or pseudo-plateau ages. An isochron age determination is not possible for any of the samples because of disturbance to all Ar spectra. Argon ages quoted in text and Table 1 are at 2σ to facilitate comparison with other data. Data were collected at 1σ and are reported as such in Appendix 3 tables.

Pb isotopes

Lead isotopic composition of galena from veins, and feldspar from plutons, was determined at the Pacific Centre for Isotopic and Geochemical Research at the University of British Columbia. Mineral separates were washed and dissolved in dilute hydrochloric acid, then prepared and analyzed using the TIMS method described by Mortensen and Gabites (2002). Errors are reported at 2σ. Data are in Table 3.

Results

Mineralogy

Breccia showings comprise recrystallized quartz-plagioclase and wall-rock fragments within quartz-muscovite-carbonate-pyrite cement cut by later, relatively simple quartz-arsenopyrite-calcite veins (Fig. 5). The quartz in these later veins is variably recrystallized. Vein showings have at least two generations of veining: 1) early recrystallized quartz-sulphide (pyrite?) veins at a high angle to foliation; and 2) veins oblique to the dominant foliation with variably recrystallized quartz-arsenopyrite-galena-pyrite (Fig. 6). In both styles of mineralization, where observed in thin section, gold is most closely associated with arsenopyrite (Fig. 4; Sack *et al.*, 2018).

U-Pb zircon geochronology

Table 1 summarizes the geochronological results for the Plateau South area.

Sample 16PS011-1 is a medium-grained, equigranular biotite-muscovite granodiorite collected from the core of the Russell stock (Fig. 2). It yielded euhedral, concentrically zoned zircons with a 3:1 aspect ratio; one grain has an inherited core (Fig. 7a). Forty-eight LA-ICPMS spot analyses yielded $^{206}Pb/^{238}U$ dates between 108 and 86 Ma, the one inherited core is 1200 Ma. The weighted mean of 41 LA-ICPMS dates is 95.95 ± 0.76 Ma (n = 41 of 48; Fig. 7b). Five zircons from 16PS011-1 were analyzed by CA-TIMS and

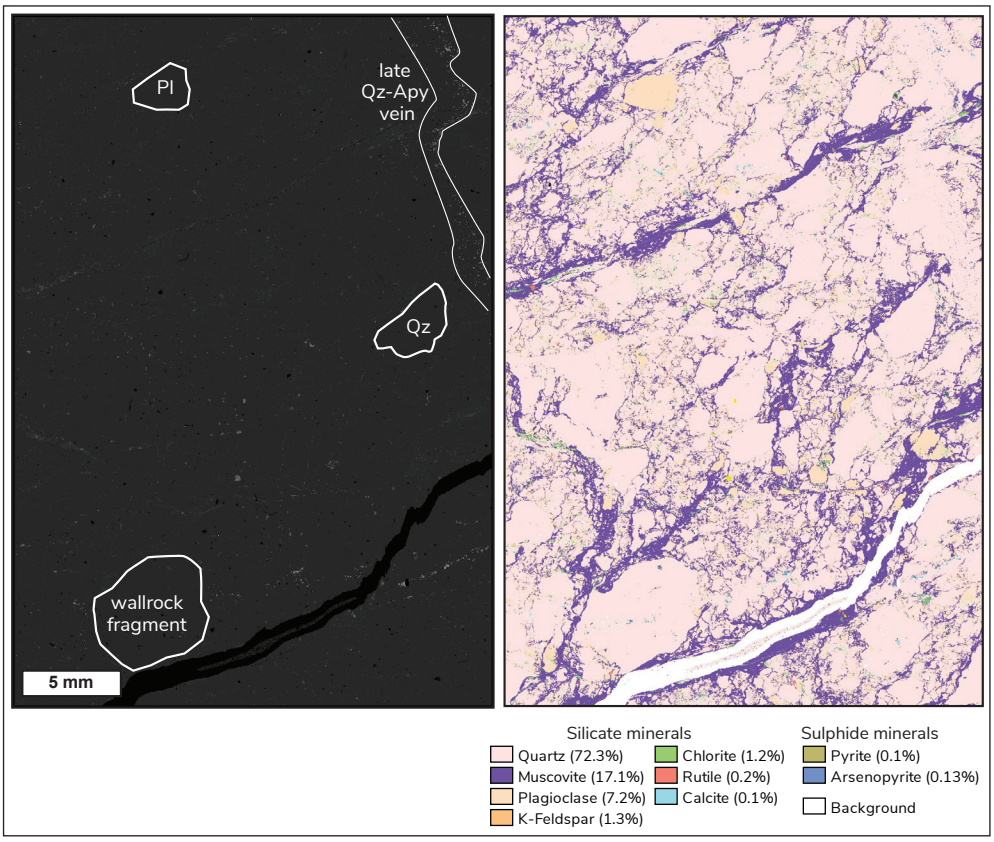

Figure 5. *Mineralogy of sample PSGS1501-31.36 m, Goldstack breccia. SEM-BSE image* ***(L)*** *and QEMSCAN particle map* ***(R)****. Minerals in the legend below QEMSCAN particle map make up 99.7% of sample by surface area. Qz = quartz, Pl = plagioclase, Apy = arsenopyrite.*

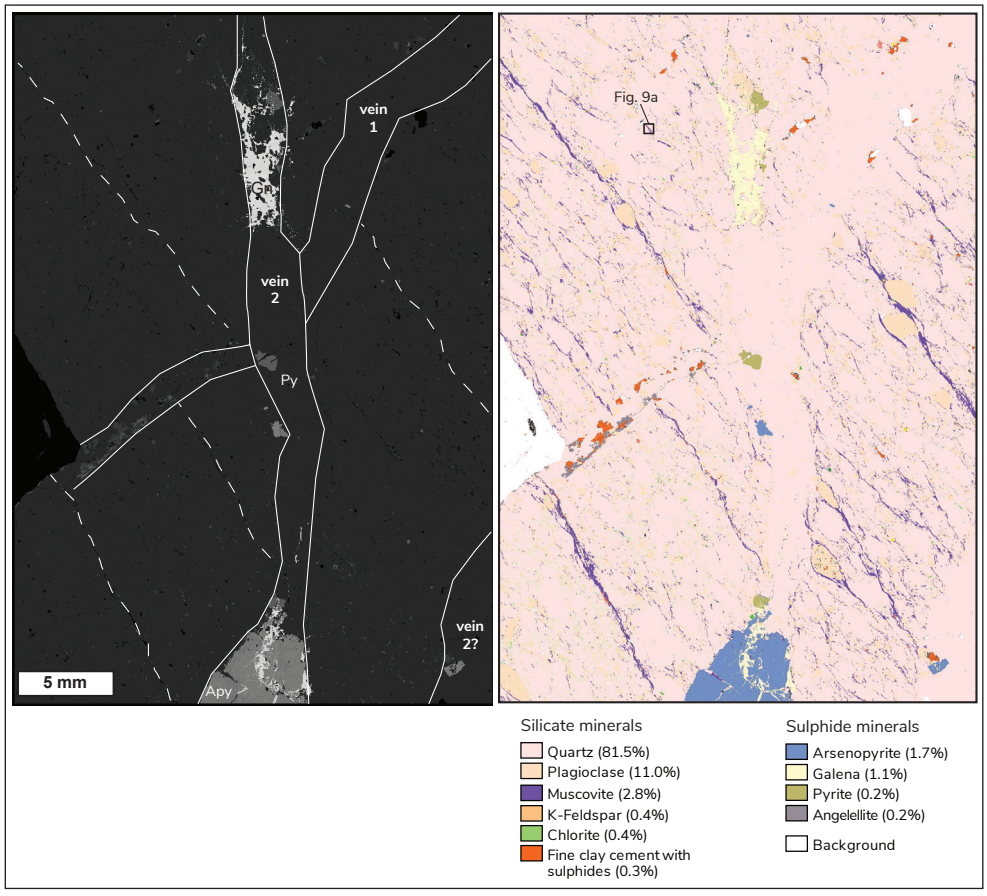

Figure 6. *Mineralogy of sample 16PS006-1, Stack West vein in the Goldbank zone. SEM-BSE image* ***(L)*** *and a QEMSCAN particle map* ***(R)****. Minerals in the legend below QEMSCAN particle map make up 99.6% of sample by surface area. Note approximate location of Fig. 9a, which is from a parallel cut thin section. Mineral abbreviations same as Fig. 5; Gn = galena.*

Table 1. *Summary table listing geochronological results.*

Sample	Zone	Showing	Latitude	Longitude	Age	Error (2σ)	MSWD	Method	Mineral	Comment	Interpretation
17PS025-1	Bullion	Bullion vein	63.345774	-133.057198	103.2	5.2	0.14	Ar/Ar	Ser	Ar loss - 77% release in 4 of 8 fractions; integrated age = 107.0±5.4	mineralization
PSGS1501-25.19m	Goldstack	Goldstack breccia	63.328847	-133.716292	130.1	6.0	0.48	Ar/Ar	Ser	excess Ar - 62% release in 4 of 8 fractions; integrated age = 196.2±5.0	regional metamorphism; possibly mineralization
17PS023-1	Bullion	Bullion schist	63.343608	-133.060891	107.0	5.2	0.84	Ar/Ar	Ms	Ar loss - 37% release in 2 of 8 fractions; integrated age = 103.9±5.0	regional metamorphism
17PS028-2	Goldbank	Ron Stack vein	63.320613	-133.475433	95.5	6.2	0.4	Ar/Ar	Ser	excess Ar - 73% release in 5 of 8 fractions; integrated age = 112.0±6.8	contact metamorphism
17PS026-1	Goldbank	Goldbank schist	63.32282	-133.508163	93.9	4.6	2.76	Ar/Ar	Ms	Ar loss - 54% release in 2 of 8 fractions; integrated age = 91.4±4.6	contact metamorphism
16PS006-1	Goldbank	Stack west vein	63.32274	-133.48071	98.8	4.0	1.8	U/Pb	Mnz	n=12; weighted mean age; small isolated grains and trains in anastomosing fabric; U/Th 0.012	regional metamorphism
16PS011-1	Russell stock	Russell stock	63.3104	-133.59449	95.4	0.03	1.3	U/Pb	Zrn	n=5 of 5; pof = 0.27; 1 inherited 1200 Ma grain	igneous crystallization
16PS013-1	Armstrong pluton	Armstrong pluton	63.25193	-133.36551	95.5	0.03	0.8	U/Pb	Zrn	n=5 of 5; pof = 0.55; no inherited grains	igneous crystallization

Ser = sericite, Ms = muscovite, Mnz = monazite, Zrn = zircon

yielded equivalent $^{206}Pb/^{238}U$ dates ranging from 95.34 ± 0.07 to 95.45 ± 0.07 Ma (Table 2), with a weighted mean age of 95.39 ± 0.03 Ma (MSWD = 1.3, n = 5; Fig. 7c). This is the best estimate of the crystallization age of the Russell stock.

Sample 16PS013-1 is a medium-grained, equigranular biotite-muscovite granite collected from an area near the north margin of the Armstrong pluton (Fig. 2). It also yielded euhedral, concentrically zoned zircons that are either stubby (~1:1 aspect ratio) or elongate (>3:1 aspect ratio; Fig. 8a). Forty-eight LA-ICPMS spot analyses yielded $^{206}Pb/^{238}U$ dates between 110 and 86 Ma; there are no inherited cores. The weighted mean of 38 LA-ICPMS dates is 93.73 ± 0.57 Ma (n = 38 of 48; Fig. 8b). Five zircons from 16PS013-1 were analyzed by CA-TIMS and yielded equivalent $^{206}Pb/^{238}U$ dates ranging from 95.54 ± 0.07 to 95.48 ± 0.07 Ma (Table 2), with a weighted mean age of 95.51 ± 0.03 Ma (MSWD = 0.8, n = 5; Fig. 8c). This is the best estimate of the crystallization age for the Armstrong pluton.

U-Th-Pb monazite geochronology

Sample 16PS006-1 is from the Stack West vein in the Goldbank area (Fig. 2) and the thin section includes both psammite wall rock and quartz-sulphide veins (Fig. 6). The *in situ* dated monazite are small (<50 µm) anhedral grains along foliation within the wall rock and are intergrown with muscovite (Figs. 6 and 9a). We interpret the monazite as metamorphic in origin. The inverse isochron age, anchored at a common-Pb $^{207}Pb/^{206}Pb$ value of 0.825 ± 0.005, for 14 of 21 analyses gives a lower intercept age of 89.8 ± 8.8 Ma (MSWD = 1.7; Fig. 9b). The ^{204}Pb-corrected weighted mean $^{208}Pb/^{232}Th$ age for 12 of these analyses is 98.8 ± 4.0 (MSWD = 1.8; Fig. 9c) which is within error of the anchored inverse isochron lower intercept age and is the best estimate for the age of regional metamorphism in the Goldbank zone.

$^{40}Ar/^{39}Ar$ geochronology

Sample 17PS023-1 is of psammitic schist that hosts veins in the Bullion zone (Fig. 2). Muscovite in this sample is predominantly related to an early bedding parallel foliation; minor new muscovite is associated

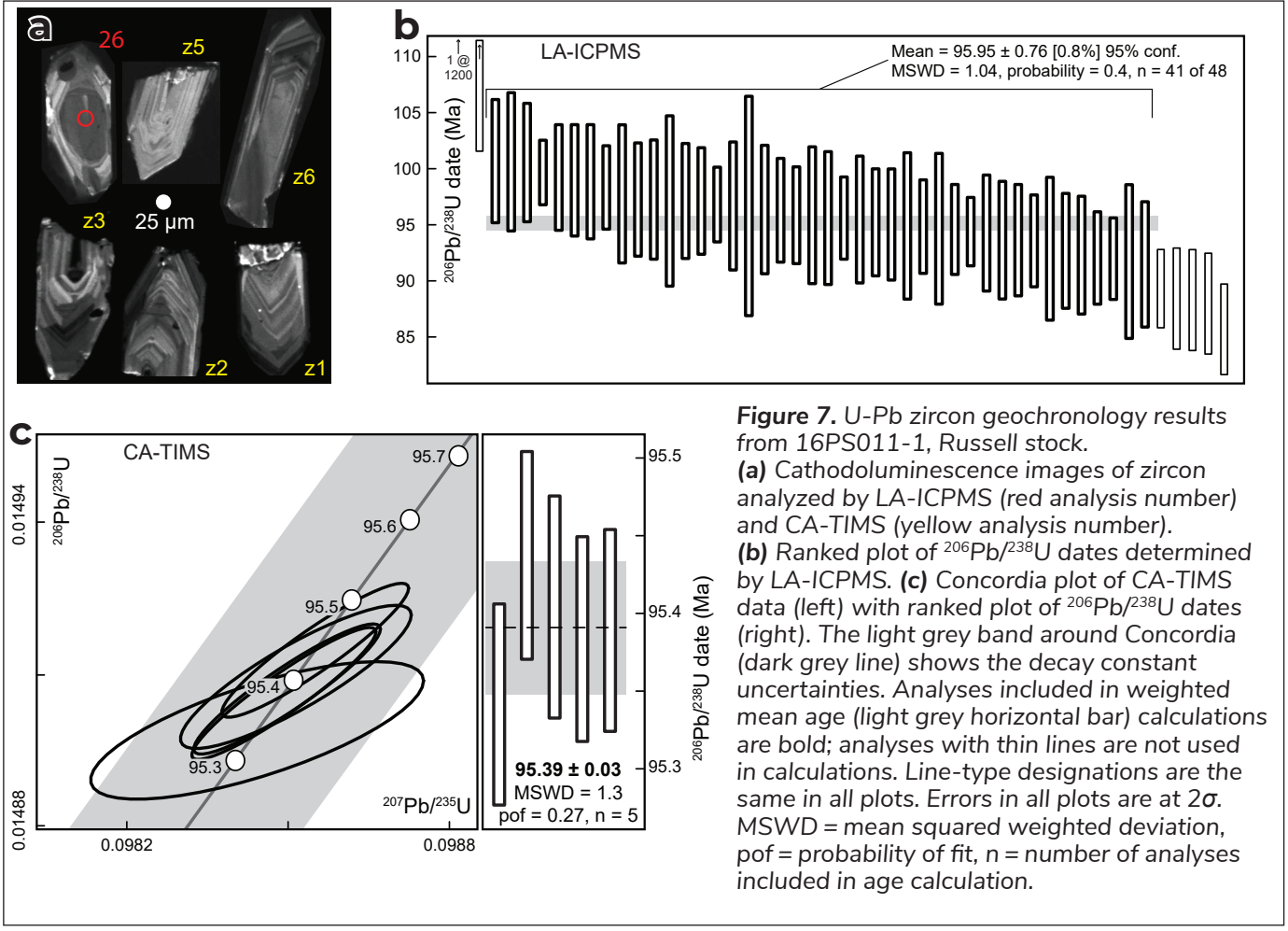

Figure 7. *U-Pb zircon geochronology results from 16PS011-1, Russell stock.* ***(a)*** *Cathodoluminescence images of zircon analyzed by LA-ICPMS (red analysis number) and CA-TIMS (yellow analysis number).* ***(b)*** *Ranked plot of ^{206}Pb/^{238}U dates determined by LA-ICPMS.* ***(c)*** *Concordia plot of CA-TIMS data (left) with ranked plot of ^{206}Pb/^{238}U dates (right). The light grey band around Concordia (dark grey line) shows the decay constant uncertainties. Analyses included in weighted mean age (light grey horizontal bar) calculations are bold; analyses with thin lines are not used in calculations. Line-type designations are the same in all plots. Errors in all plots are at 2σ. MSWD = mean squared weighted deviation, pof = probability of fit, n = number of analyses included in age calculation.*

with a subsequent foliation. A muscovite separate gave an integrated age of 103.9 ± 5.0 Ma and a weighted mean age from two overlapping, but non-sequential, steps of 107.6 ± 5.2 Ma (2 of 8 steps, 36.9% ^{39}Ar release MSWD = 0.84; Fig. 10). The spectra have a 'stepping-up' age pattern where the higher temperature steps had older ages than the lower temperature steps. This pattern is indicative of gas loss due to alteration or reheating and suggests the oldest step (109.65 ± 0.8 Ma) may be a minimum age. The spectra do not meet the sequential overlapping criteria for a plateau age; hence, a weighted average age of steps 6 and 8 is presented. The integrated and weighted average age are within error of each other. We interpret the weighted average age of 107.0 ± 5.2 Ma as the minimum age of significant regional metamorphism recording the end of ductile deformation and metamorphism ca. 110 to 105 Ma.

Sample 17PS026-1 is psammitic schist that hosts veins in the Goldbank zone (Fig. 2). The same two generations of muscovite recognized in 17PS023-1 are also recognized in this sample. A muscovite separate gave an integrated age for all steps of 91.4 ± 4.6 Ma and a pseudo-plateau age of 93.7 ± 7.0 Ma (3 of 8 steps, 63.6% ^{39}Ar release MSWD = 2.19; Fig. 10). The spectra have a 'stepping-up' age pattern indicative of gas loss due to alteration or reheating. The integrated and pseudo-plateau ages are within error. We interpret the plateau age of 93.7 ± 7.0 Ma as reset by the nearby 95.5 Ma intrusions.

Sample PSGS1501-25.19m is from a mineralized and recrystallized quartz-sericite-sulphide breccia in the Goldstack area. A sericite separate from the sample gave an integrated age for all steps of 196.2 ± 5.0 Ma and a plateau age of 130.1 ± 6.0 Ma (4 of 8 steps, 62.3% ^{39}Ar release MSWD = 0.48; Fig. 11).

Table 2. *CA-TIMS U-Pb zircon data table. The data and calculations for this table are available in Appendix 2.*

Sample	Th/U	$^{206}Pb^*$ x10^{-13} mol	mol% $^{206}Pb^*$	Pb^*/Pb_c	Pb_c (pg)	$^{206}Pb/^{204}Pb$	$^{208}Pb/^{206}Pb$	$^{207}Pb/^{206}Pb$	% err	$^{207}Pb/^{235}U$	% err	$^{206}Pb/^{238}U$	% err	corr. coef.	$^{207}Pb/^{206}Pb$	±	$^{207}Pb/^{235}U$	±	$^{206}Pb/^{238}U$	±	include in weighted mean
(a)	(b)	(c)	(c)	(c)	(c)	(d)	(e)	(e)	(f)	(e)	(f)	(e)	(f)		(g)	(f)	(g)	(f)	(g)	(f)	
16PS11-1																					
z1	0.226	2.7152	99.84%	177.9	0.35	11647	0.072	0.0480	0.080	0.0986	0.142	0.0149	0.071	0.940	98.14	1.90	95.49	0.13	95.38	0.07	x
z2	0.403	2.0437	99.86%	210.3	0.24	13030	0.129	0.0480	0.082	0.0987	0.144	0.0149	0.072	0.932	99.59	1.93	95.61	0.13	95.45	0.07	x
z3	0.456	1.1147	99.65%	85.8	0.32	5269	0.146	0.0480	0.118	0.0986	0.178	0.0149	0.077	0.867	97.48	2.79	95.49	0.16	95.41	0.07	x
z5	0.565	0.6973	99.55%	68.2	0.26	4066	0.181	0.0479	0.210	0.0985	0.257	0.0149	0.074	0.719	96.08	4.97	95.36	0.23	95.34	0.07	x
z6	0.312	2.6767	99.91%	303.3	0.21	19223	0.100	0.0480	0.084	0.0986	0.144	0.0149	0.070	0.923	98.46	1.98	95.51	0.13	95.39	0.07	x
16PS13-1																					
z1	0.250	8.0530	99.97%	955.7	0.20	61561	0.080	0.0480	0.065	0.0987	0.129	0.0149	0.070	0.965	97.13	1.53	95.60	0.12	95.54	0.07	x
z2	0.200	6.8267	99.96%	719.7	0.22	47103	0.064	0.0480	0.065	0.0987	0.130	0.0149	0.071	0.966	97.75	1.53	95.59	0.12	95.50	0.07	x
z3	0.251	5.9637	99.96%	663.5	0.21	42764	0.080	0.0480	0.067	0.0988	0.131	0.0149	0.071	0.960	98.52	1.58	95.65	0.12	95.54	0.07	x
z5	0.354	2.9896	99.90%	294.8	0.24	18516	0.113	0.0480	0.079	0.0987	0.140	0.0149	0.070	0.937	97.69	1.86	95.56	0.13	95.48	0.07	x
z6	0.387	2.8976	99.89%	274.2	0.26	17079	0.124	0.0480	0.079	0.0987	0.141	0.0149	0.071	0.936	97.85	1.87	95.57	0.13	95.48	0.07	x

(a) z1, z2, etc. are labels for analyses composed of single zircon grains that were annealed and chemically abraded (Mattinson, 2005). Labels in bold denote analyses used in weighted mean calculations or discordia regressions.
(b) Model Th/U ratio calculated from radiogenic $^{208}Pb/^{206}Pb$ ratio and $^{207}Pb/^{235}U$ date.
(c) Pb* and Pbc are radiogenic and common Pb, respectively. mol% $^{206}Pb^*$ is with respect to radiogenic and blank Pb.
(d) Measured ratio corrected for spike and fractionation only. Fractionation correction is 0.16 ± 0.03 (1 sigma) %/amu (atomic mass unit) for single-collector Daly analyses, based on analysis of EARTHTIME 202Pb-205Pb tracer solution.
(e) Corrected for fractionation and spike. Common Pb in zircon analyses is assigned to procedural blank with composition of $^{206}Pb/^{204}Pb$ = 18.04 ± 0.61%; $^{207}Pb/^{204}Pb$ = 15.54 ± 0.52%; $^{208}Pb/^{204}Pb$ = 37.69 ± 0.63% (1 sigma). $^{206}Pb/^{238}U$ and $^{207}Pb/^{206}Pb$ ratios corrected for initial disequilibrium in $^{230}Th/^{238}U$ using a D(Th/U) of 0.20 ± 0.05 (1 sigma).
(f) Errors are 2 sigma, propagated using algorithms of Schmitz and Schoene (2007) and Crowley et al. (2007).
(g) Calculations based on the decay constants of Jaffey et al. (1971). $^{206}Pb/^{238}U$ and $^{207}Pb/^{206}Pb$ dates corrected for initial disequilibrium in $^{230}Th/^{238}U$ usinga D(Th/U) of 0.20 ± 0.05 (1 sigma).

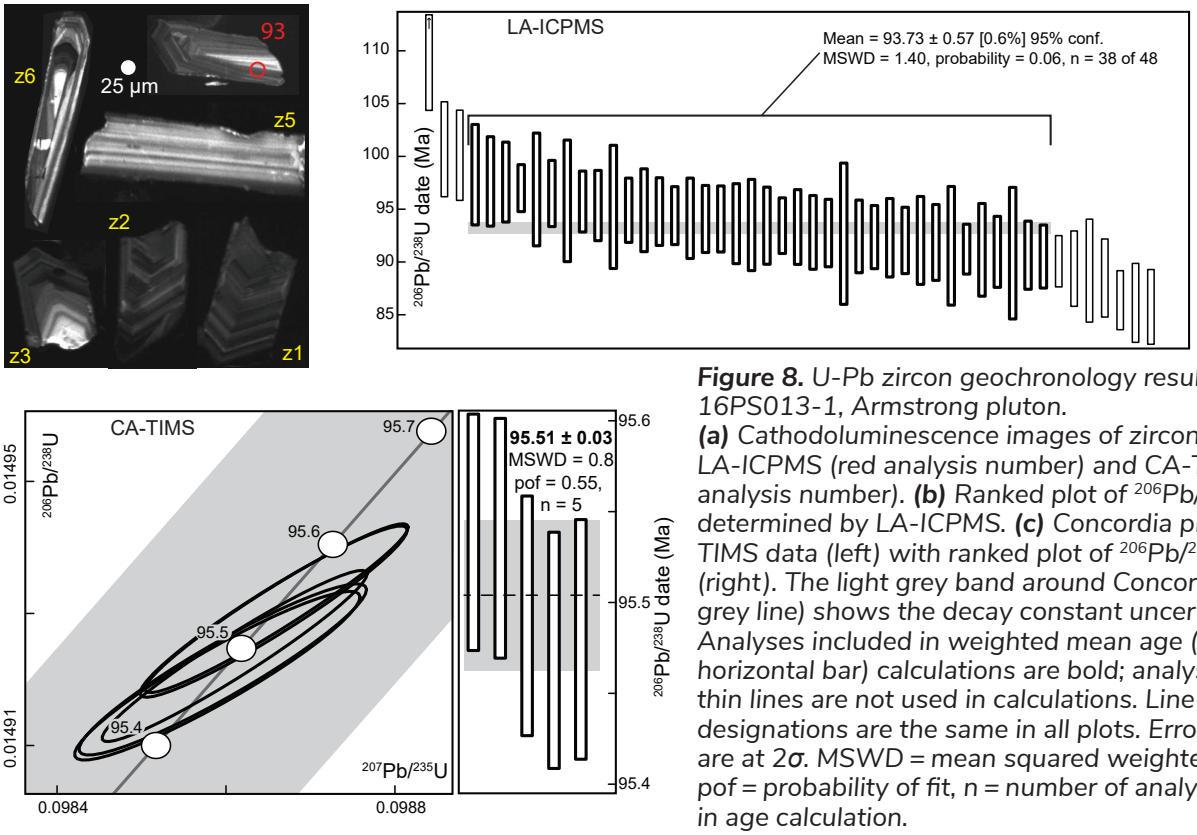

Figure 8. *U-Pb zircon geochronology results from 16PS013-1, Armstrong pluton.* ***(a)*** *Cathodoluminescence images of zircon analyzed by LA-ICPMS (red analysis number) and CA-TIMS (yellow analysis number).* ***(b)*** *Ranked plot of $^{206}Pb/^{238}U$ dates determined by LA-ICPMS.* ***(c)*** *Concordia plot of CA-TIMS data (left) with ranked plot of $^{206}Pb/^{238}U$ dates (right). The light grey band around Concordia (dark grey line) shows the decay constant uncertainties. Analyses included in weighted mean age (light grey horizontal bar) calculations are bold; analyses with thin lines are not used in calculations. Line-type designations are the same in all plots. Errors in all plots are at 2σ. MSWD = mean squared weighted deviation, pof = probability of fit, n = number of analyses included in age calculation.*

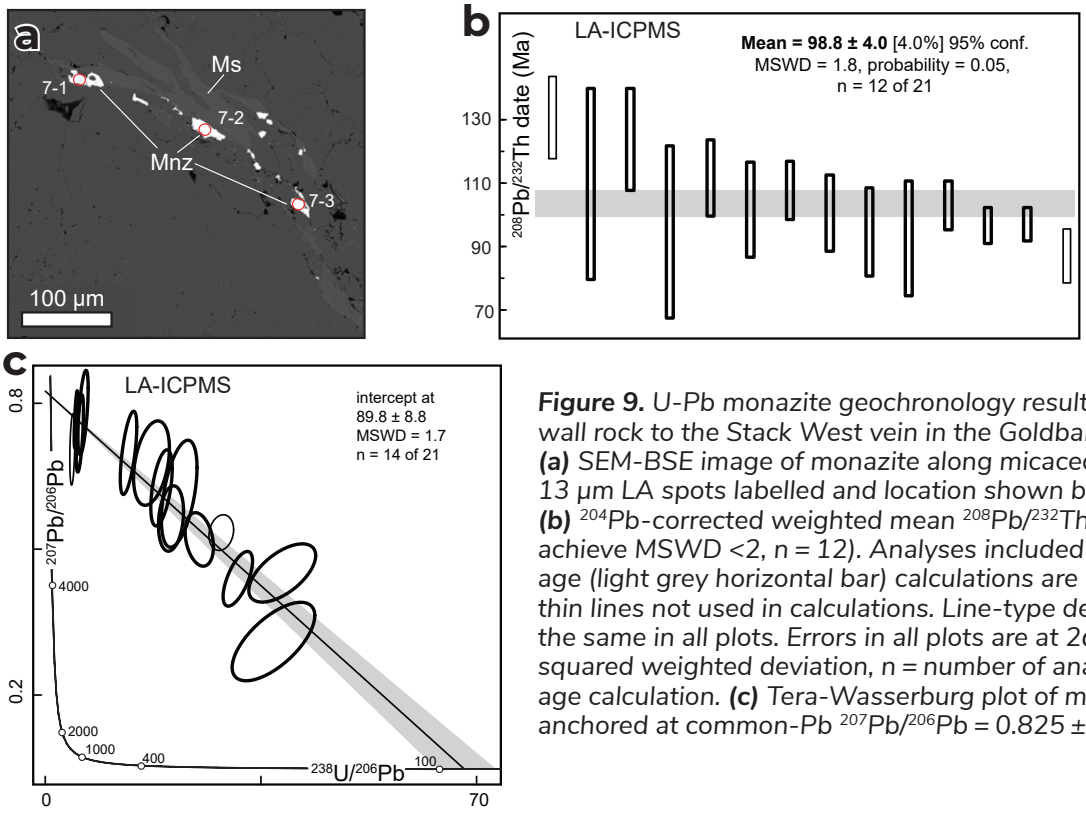

Figure 9. *U-Pb monazite geochronology results from 16PS006-1, wall rock to the Stack West vein in the Goldbank zone.* ***(a)*** *SEM-BSE image of monazite along micaceous foliation plane; 13 µm LA spots labelled and location shown by open red circle.* ***(b)*** *^{204}Pb-corrected weighted mean $^{208}Pb/^{232}Th$ age (refined to achieve MSWD <2, n = 12). Analyses included in weighted mean age (light grey horizontal bar) calculations are bold; analyses with thin lines not used in calculations. Line-type designations are the same in all plots. Errors in all plots are at 2σ. MSWD = mean squared weighted deviation, n = number of analyses included in age calculation.* ***(c)*** *Tera-Wasserburg plot of monazite data, n = 14, anchored at common-Pb $^{207}Pb/^{206}Pb = 0.825 \pm 0.005$.*

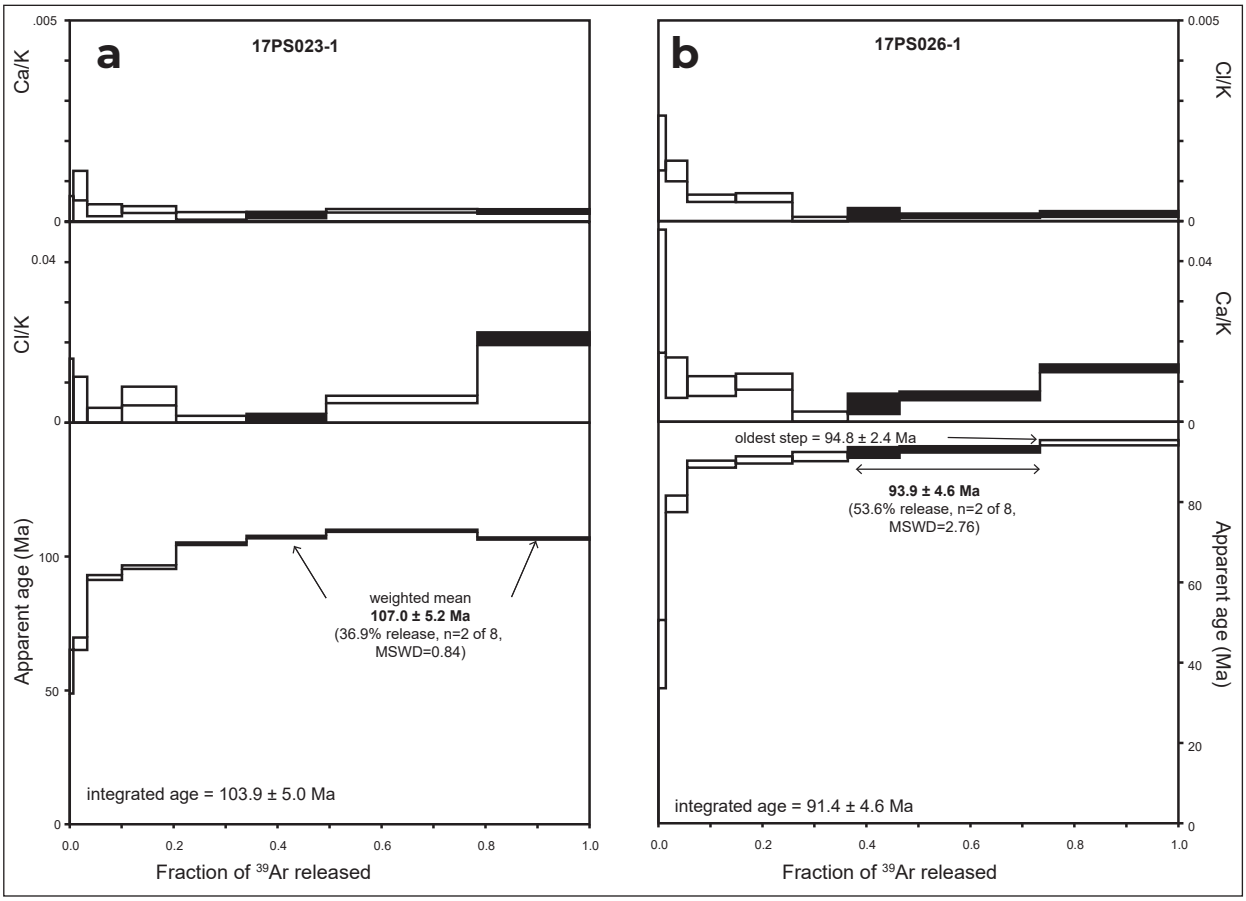

Figure 10. *^{40}Ar/^{39}Ar spectra for muscovite from schist in the* ***(a)*** *Bullion zone, 17PS023-1, and* ***(b)*** *Goldbank zone, 17PS026-1. Steps in black were used to calculate the age.*

Excess Ar released in the youngest and oldest steps have resulted in anomalously old ages (up to 1.4 billion years old) and therefore the Ar spectra is 'U-shaped'. This showing exhibits strongly recrystallized quartz suggesting the sericite in the sample was also recrystallized and mineralization was pre to syn-deformation. Due to the unquantifiable influence of excess Ar we interpret the age of this sample as a maximum age; the actual age could be significantly younger.

Sample 17PS025-1 is from a vein in the Bullion zone. A sericite separate from the sample gave an integrated age for all steps of 107.0 ± 5.4 Ma and a plateau age of 103.2 ± 5.2 Ma (4 of 8 steps, 77.1% ^{39}Ar release MSWD = 0.14; Fig. 11). The spectra have a 'stepping-up' age pattern indicative of gas loss. The integrated and plateau ages are within error. We interpret the plateau age of 103.2 ± 5.2 Ma as the age of mineralization in this sample.

Sample 17PS028-2 is from the Ron Stack vein, Goldbank zone. A sericite separate gave an integrated age for all steps of 112.0 ± 6.8 Ma and a plateau age of 95.5 ± 6.2 Ma (5 of 8 steps, 72.8% ^{39}Ar release MSWD = 0.40; Fig. 11). The spectra have a slight 'U-shaped' age pattern indicative of excess Ar. The integrated and the plateau ages are not within error. We interpret the plateau age of 95.5 ± 6.2 Ma as a maximum age, due to either resetting by contact metamorphism or reflecting mineralization, an interpretation elaborated on in the discussion.

Pb isotopes

Radiogenic Pb isotopes ^{206}Pb, ^{207}Pb and ^{208}Pb were analyzed from galena in eight vein samples and feldspar from four pluton samples; two vein samples and one pluton were analyzed twice (Table 3). Two groupings are apparent in the data, (1) a more isotopically primitive,

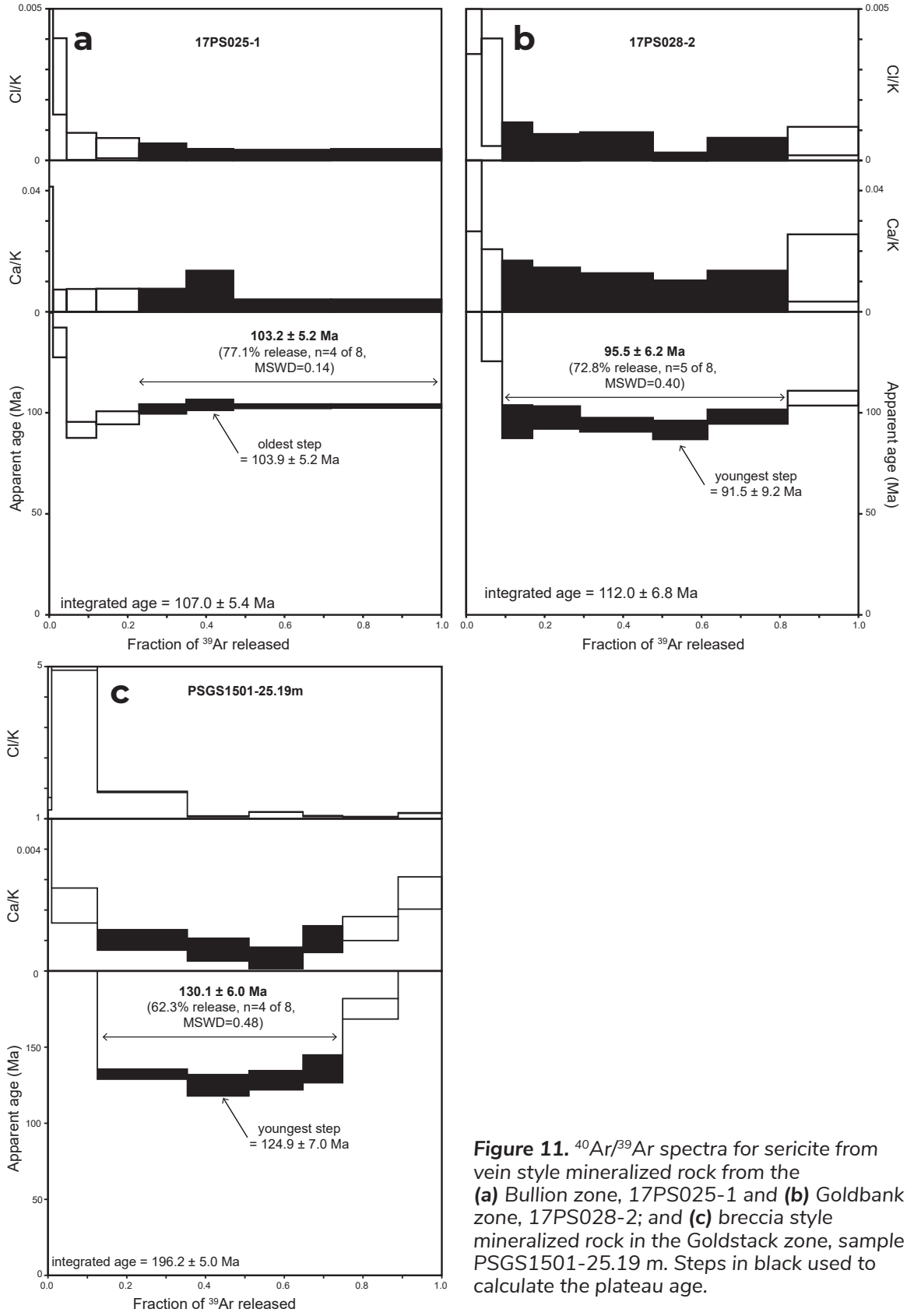

Figure 11. *$^{40}Ar/^{39}Ar$ spectra for sericite from vein style mineralized rock from the* ***(a)*** *Bullion zone, 17PS025-1 and* ***(b)*** *Goldbank zone, 17PS028-2; and* ***(c)*** *breccia style mineralized rock in the Goldstack zone, sample PSGS1501-25.19 m. Steps in black used to calculate the plateau age.*

Table 3. Lead isotope data table.

Sample	Zone	Showing	Grp	Latitude	Longitude	Mineral	$^{206}Pb/^{204}Pb$	Error abs (2σ)	$^{207}Pb/^{204}Pb$	Error abs (2σ)	$^{208}Pb/^{204}Pb$	Error abs (2σ)	$^{207}Pb/^{206}Pb$	Error abs (2σ)	$^{208}Pb/^{206}Pb$	Error abs (2σ)
17PS017-1	Big Bang vein	Big Bang	1	63.3739	-133.9397	Gn	18.301	0.0004	15.581	0.0002	38.499	0.0008	0.8514	0.0000	2.104	0.0000
17PS018-1	Big Bang vein	Big Bang	1	63.3882	-133.9379	Gn	18.135	0.0029	15.555	0.0024	38.302	0.0062	0.8577	0.0000	2.112	0.0001
16PS007-3	Bonanza vein	Bonanza	1	63.3555	-133.7555	Gn	18.309	0.0028	15.618	0.0020	38.512	0.0064	0.8530	0.0001	2.103	0.0002
Goldstack01	Goldstack	Goldstack breccia	1	63.3291	-133.7162	Gn	18.168	0.0048	15.569	0.0029	38.772	0.0114	0.8569	0.0002	2.134	0.0003
Goldstack01	Goldstack	Goldstack breccia	1	63.3291	-133.7162	Gn	18.146	0.0021	15.559	0.0017	38.731	0.0050	0.8574	0.0000	2.134	0.0001
17PS027-1	Goldbank	Astro vein	2	63.3215	-133.4782	Gn	19.035	0.0012	15.712	0.0007	39.189	0.0029	0.8254	0.0000	2.059	0.0001
17PS028-3	Goldbank	Lewis vein	2	63.3206	-133.4754	Gn	19.112	0.0007	15.729	0.0005	39.299	0.0016	0.8230	0.0000	2.056	0.0000
16PS006-1	Goldbank	Stack west vein	2	63.3227	-133.4807	Gn	19.010	0.0015	15.728	0.0007	39.225	0.0033	0.8273	0.0001	2.063	0.0001
PSGR1702-20m	Goldbank	Gold Bar vein	2	63.3336	-133.5486	Gn	18.939	0.0061	15.656	0.0044	39.100	0.0141	0.8267	0.0001	2.065	0.0003
PSGR1702-20m	Goldbank	Gold Bar vein	2	63.3336	-133.5486	Gn	18.911	0.0013	15.679	0.0010	39.142	0.0032	0.8291	0.0000	2.070	0.0001
16PS013	Armstrong pluton	Armstrong pluton	2	63.2519	-133.3655	Kfs	19.245	0.0015	15.696	0.0007	39.204	0.0043	0.8156	0.0000	2.037	0.0002
16PS015	Armstrong pluton	Armstrong pluton	2	63.2654	-133.3672	Kfs	19.145	0.0142	15.626	0.0115	39.069	0.0291	0.8162	0.0001	2.041	0.0002
16PS009	Russell stock	Russell stock	2	63.2915	-133.6063	Kfs	19.323	0.0222	15.775	0.0174	39.442	0.0464	0.8164	0.0003	2.041	0.0005
16PS009	Russell stock	Russell stock	2	63.2915	-133.6063	Kfs	19.358	0.0157	15.765	0.0107	39.375	0.0335	0.8144	0.0004	2.034	0.0005
16PS11	Russell stock	Russell stock	2	63.3104	-133.5945	Kfs	19.244	0.0068	15.726	0.0054	39.328	0.0140	0.8172	0.0001	2.044	0.0001

abs = absolute

thorogenic Pb-enriched group of five analyses that clusters along the 'orogene curve' of Zartman and Doe (1981), and (2) a more isotopically evolved group of 10 analyses which clusters around the 'Selwyn shale curve' of Godwin and Sinclair (1982). Group 1 comprises galena from mineralized rocks in the Goldstack, Bonanza and Big Bang zones on the western side of the property and has $^{206}Pb/^{204}Pb$ values between 18.31 and 18.14, $^{207}Pb/^{204}Pb$ between 15.62 and 15.55 and $^{208}Pb/^{204}Pb$ between 38.77 and 38.30 (Table 3). Group 2 comprises galena from the Goldbank zone as well as feldspar from the Russell and Armstrong plutons and has $^{206}Pb/^{204}Pb$ values between 19.13 and 18.91, $^{207}Pb/^{204}Pb$ between 15.78 and 15.63 and $^{208}Pb/^{204}Pb$ between 39.24 and 39.07 (Table 3).

Discussion

Tungsten plutonic suite

The Russell stock and Armstrong pluton have previously been assigned to the Tombstone suite (Roots, 2003) and Mayo suite (Rasmussen, 2013). Roots (1998) described the plutons in the Lansing map sheet area (105N) as biotite dominant over hornblende granodiorite intrusions of mid-Cretaceous age. Mid-Cretaceous plutons in the Selwyn basin area share many similarities and suites are challenging to separate (Rasmussen, 2013). In fact, the *ca.* 98 to 90 Ma Tungsten, Mayo, and Tombstone suite plutons are often referred to together as the Tungsten - Tombstone belt (*e.g.*, TTB in Hart *et al.*, 2004). The ages of these three suites are close, and mineralogy and geochemistry are useful for differentiating the suites (Hart *et al.*, 2004; Rasmussen, 2013). Tungsten suite plutons (98 to 94 Ma) are biotite ± hornblende ± muscovite ± garnet intermediate plutons with low magnetic character (0.2×10^{-3} SI units) and are peraluminous. Mayo suite plutons (96 to 93 Ma) are hornblende ± biotite intermediate plutons with low magnetic character (0.1×10^{-3} SI units) and are metaluminous. Tombstone suite plutons (92 to 90 Ma) are hornblende ± biotite intermediate plutons with moderate magnetic character (1.8×10^{-3} SI units) and are mainly metaluminous with fewer examples of peralkaline and peraluminous intrusions.

We did not observe hornblende in four thin sections from the Russell and Armstrong plutons and noted only minor hornblende in the field (Sack *et al.*, 2018). Both plutons have similar geochemistry and are ferroan, calcic and peraluminous using the criteria of Frost *et al.* (2001; Fig. 12). These characteristics combined with the presence of minor muscovite and garnet and the new 95.5 Ma ages presented in this paper, better match the description of the Tungsten suite in Rasmussen (2013). The tungsten skarn occurrence (Tongue, Yukon MINFILE 105N 014) on the south margin of the Armstrong pluton is another hallmark of Tungsten suite intrusions (Rasmussen, 2013). We suggest reassigning the Russell stock and Armstrong pluton to the Tungsten suite. This would make these intrusions the farthest west examples of the Tungsten suite.

Plateau breccia and vein showings

Quantitative mineralogy confirms thin section observations that both vein and breccia style showings have at least two generations of mineralization, both of which seem to have been recrystallized to some extent. The vein mineralogy and paragenesis is similar for both styles and based on these characteristics the two types seem best described as structural variations on the same veining event(s).

The age of mineralization at the Plateau South property is an important constraint on the deposit model used to describe mineralization (Sack *et al.*, 2018). While the U-Pb zircon data presented here are considered easy to interpret, the U-Pb monazite and Ar data are less so; with that in mind, we identify two events in the geochronologic data (Fig. 13). The oldest is a protracted period of orogenic mineralization and metamorphism from a maximum of *ca.* 130 Ma to *ca.* 100 Ma. Shortly afterwards, there is a well-constrained intrusive event at 95.5 Ma with coeval mineralization or thermal resetting of sericite in veins near plutons. Our monazite and muscovite geochronologic data suggest that the end of ductile deformation in the Plateau area was *ca.* 110 to 100 Ma. Ductile deformation and regional metamorphism were complete by 95.5 Ma when undeformed cordierite and andalusite porphyroblasts associated with intrusion of the Russell stock overgrew regional metamorphic fabrics (Fig. 3; Sack *et al.*, 2018).

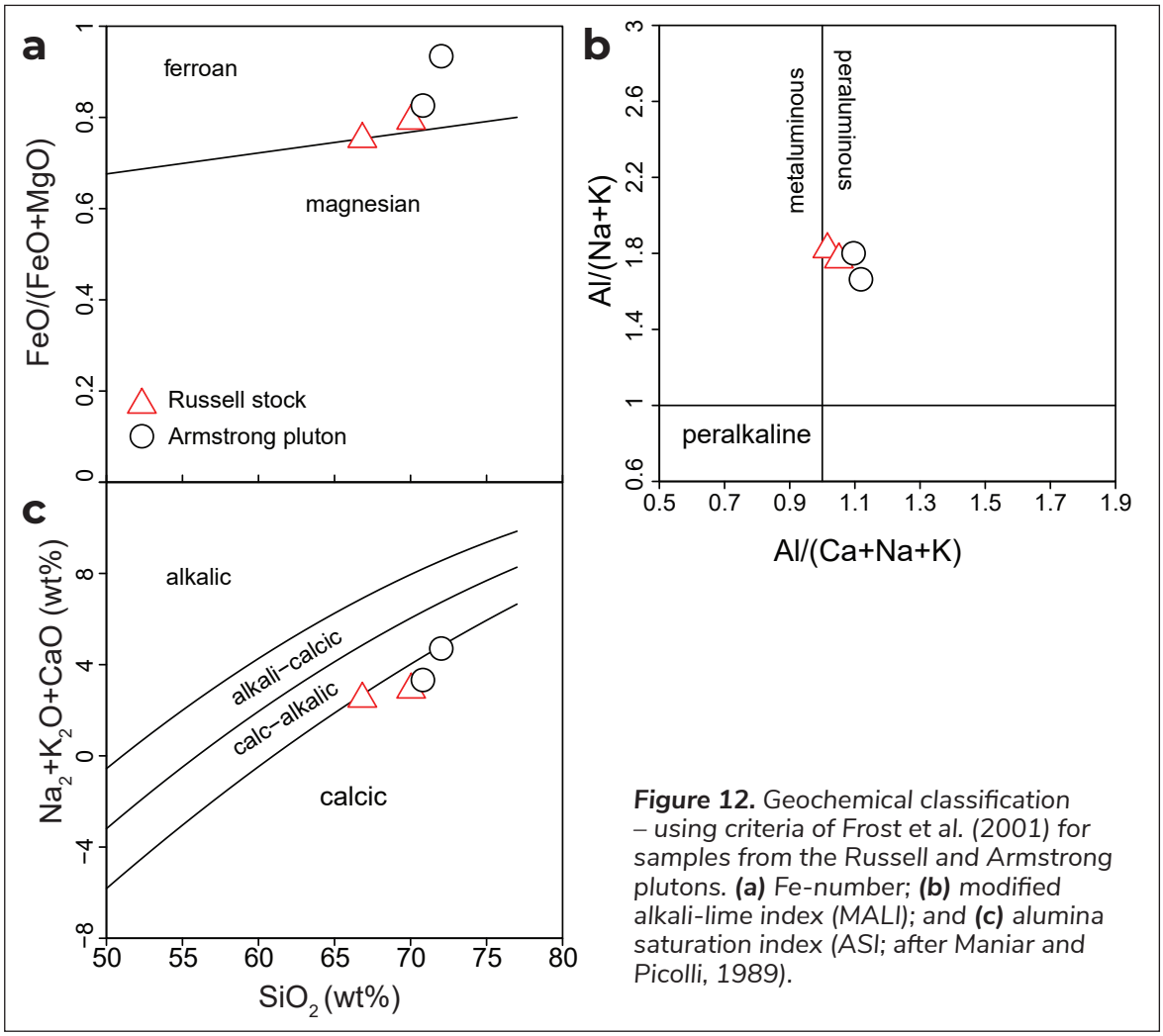

Figure 12. *Geochemical classification – using criteria of Frost et al. (2001) for samples from the Russell and Armstrong plutons.* ***(a)*** *Fe-number;* ***(b)*** *modified alkali-lime index (MALI); and* ***(c)*** *alumina saturation index (ASI; after Maniar and Picolli, 1989).*

This late Early Cretaceous end to regional metamorphism is relatively consistent throughout the Selwyn basin area (Fig. 1). For example, in the Hyland area 112 Ma dikes are deformed whereas, 106 Ma intrusions (Heffernan and Mortensen, 2000) are undeformed (Moynihan pers comm, 2019). In the Anvil area 50 km south of Plateau, deformation is constrained to as young as ca. 109 to 104 Ma based on early Anvil batholith dikes that are weakly deformed and weak foliation in parts of the Anvil batholith (Pigage, 2004). In the McQuesten area, $^{40}Ar/^{39}Ar$ cooling ages of ca. 104 to 100 Ma metamorphic muscovite provide a lower age constraint for Tombstone strain zone deformation (Mair et al., 2006). The onset of Jura-Cretaceous deformation is less well constrained throughout the Selwyn basin area of Yukon. The nearest reliable estimate is from *in situ* monazite dating in the Finlayson Lake area, 300 km southeast of the Plateau area, where the regional metamorphic age is as young as 142 Ma (Staples et al., 2014). For comparison, the Cariboo and Sheep Creek orogenic gold camps of southern British Columbia have regional metamorphic ages of Late Jurassic to Early Cretaceous and protracted orogenic mineralization ages from ca. 143 Ma to 133 Ma (Allan et al., 2017). We suggest a similar sequence of events in the Plateau area though we interpret our data as indicating a slightly younger Early Cretaceous (ca. 130 to 100 Ma) orogenic mineralization event.

The Pb isotopic composition of sulphides precipitated from magmatic or hydrothermal fluids reflects the Pb isotopic composition of the metal source(s) (Tosdal et al., 1999) and thus helps constrain genetic models.

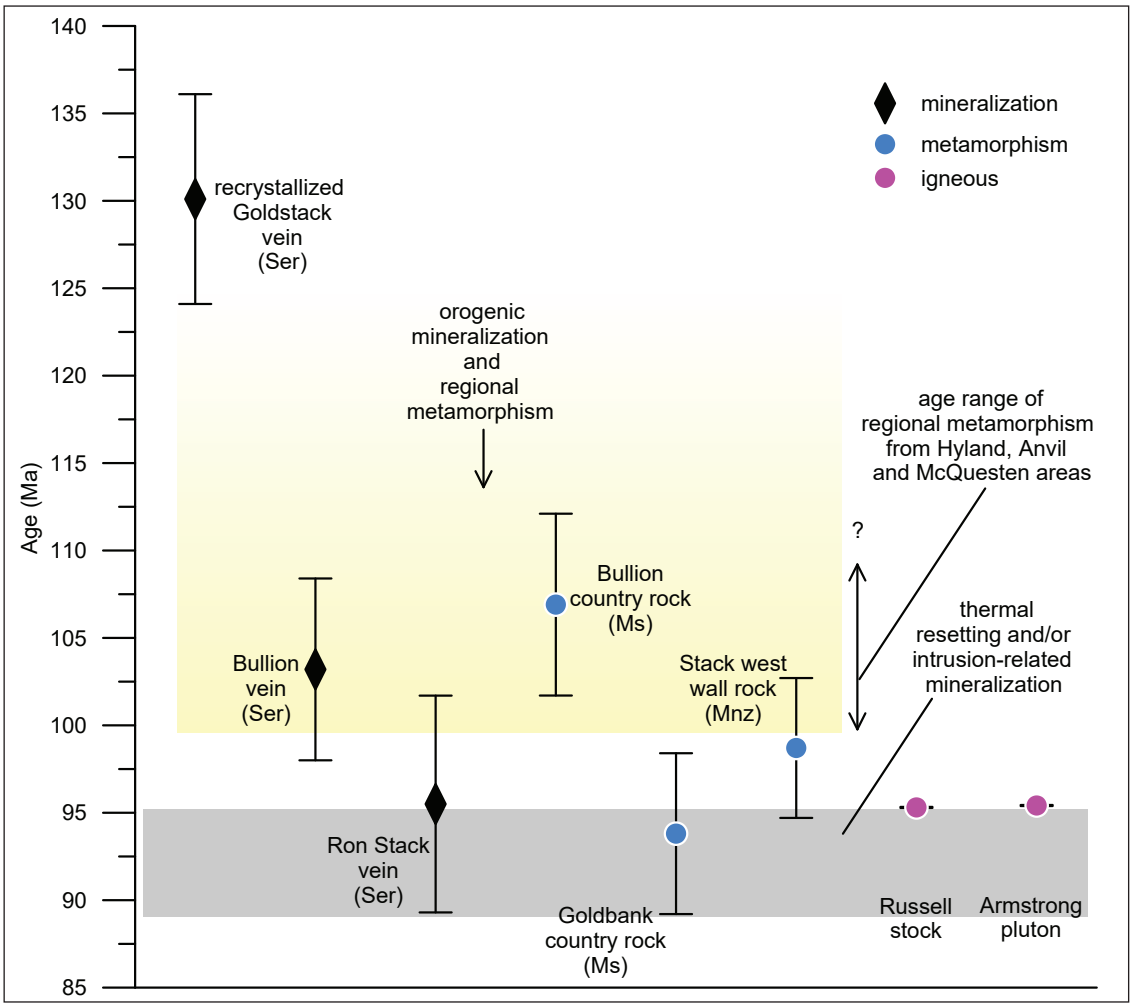

Figure 13. *Geochronology summary for the Plateau area. Regional metamorphism for the Hyland area from Moynihan (pers. comm), the Anvil area from Pigage (2004) and the McQuesten area from Mair et al. (2006). Errors 2σ.*

For example, in intrusion-related systems, the sulphide Pb isotopic composition is similar to those of igneous feldspar within genetically related intrusions (Tosdal et *al.*, 1999). The close spatial and genetic association between galena and arsenopyrite and arsenopyrite and gold in the Plateau occurrences (Sack et *al.*, 2018) suggests Pb, As and Au were in the same hydrothermal fluid and Pb is a useful proxy for gold source at Plateau. We do note that while the paragenesis of galena in discrete vein showings is relatively well constrained to later than arsenopyrite, similar constraints are not known for the breccia showings.

One breccia showing, and two vein showings on the western side of the property are enriched in thorogenic Pb (Group 1) indicative of Pb sources from relatively isotopically primitive rocks (Zartman and Doe, 1981; Tosdal et *al.*, 1999). This may indicate the early orogenic mineralizing fluids were sourced relatively deep in the lower crust, the 'orogene' of Zartman and Doe (1981), or that they interacted locally with rocks such as the mafic volcanic Old Cabin Formation. The Pb isotopic signature from primitive rocks is relatively easily overwhelmed by evolved rocks due to lower Pb concentrations overall in primitive rocks (Tosdal et *al.*, 1999). Whole-rock Pb for one sample from the chloritic phyllite in the Big Bang area is <5 ppm (detection limit), country rocks are between 7 and 26 ppm Pb, and intrusions have 30 to 42 ppm Pb (Appendix 1). This suggests that the Group 1 Pb signature is from fluid that did not interact with the relatively Pb-rich country rock or intrusions.

The Pb isotope signature of vein showings in the Big Bang area (Group 2) is distinct from Group 1. Group 2 Pb isotopic data are similar to that of feldspar in mid-Cretaceous intrusions of the Selwyn basin area and to the country rocks (Fig. 14). Data from the Russell and Armstrong plutons overlap entirely with that of other mid-Cretaceous plutons across the Selwyn basin area (Fig. 14). Country rock Pb isotopic composition for the Selwyn basin area is best estimated from syngenetic massive sulphide deposits throughout the stratigraphy and is presented as the 'Selwyn shale' curve of Godwin and Sinclair (1982). These data are corroborated by limited whole-rock Pb isotopic data from widespread samples of Yusezyu Formation shale (Ben Cave written comm., 2018). The similar Pb isotopic composition for mid-Cretaceous plutons and country rock suggests a fundamental, regional basement control on the composition of lead in the area. From the point of view of mineralization at Plateau, it is not possible to distinguish between plutons and country rock as a source of Pb in hydrothermal fluids. Thus, the more isotopically evolved signature is compatible with metals sourced from either the plutons or the country rock. However, it is worth restating, that Pb isotopic data show two distinct sources of Pb in the Plateau deposits and any genetic model must account for this.

The above data are internally consistent in that each data set suggests at least two mineralizing events: (1) mineralogy and petrography show at least two stages of veining or brecciation; (2) geochronologic data broadly cluster into two ranges; and (3) Pb isotopic data clearly show two distinct metal sources. Unfortunately, these data do not allow a unique solution as to which deposit model best explains mineralization on the Plateau property. Below, we present what we consider the two most likely options.

1. Initial mineralization relates to Early Cretaceous (ca. 130 to 100 Ma) orogenic fluids and later mineralization is intrusion-related (ca. 95 Ma). In this interpretation, Early Cretaceous regional-scale orogenic fluids are envisioned to have tapped a primitive (deep?) Pb source with minimal interaction with surrounding rocks and intrusion-related mineralization sourced Pb from mid-Cretaceous plutons.

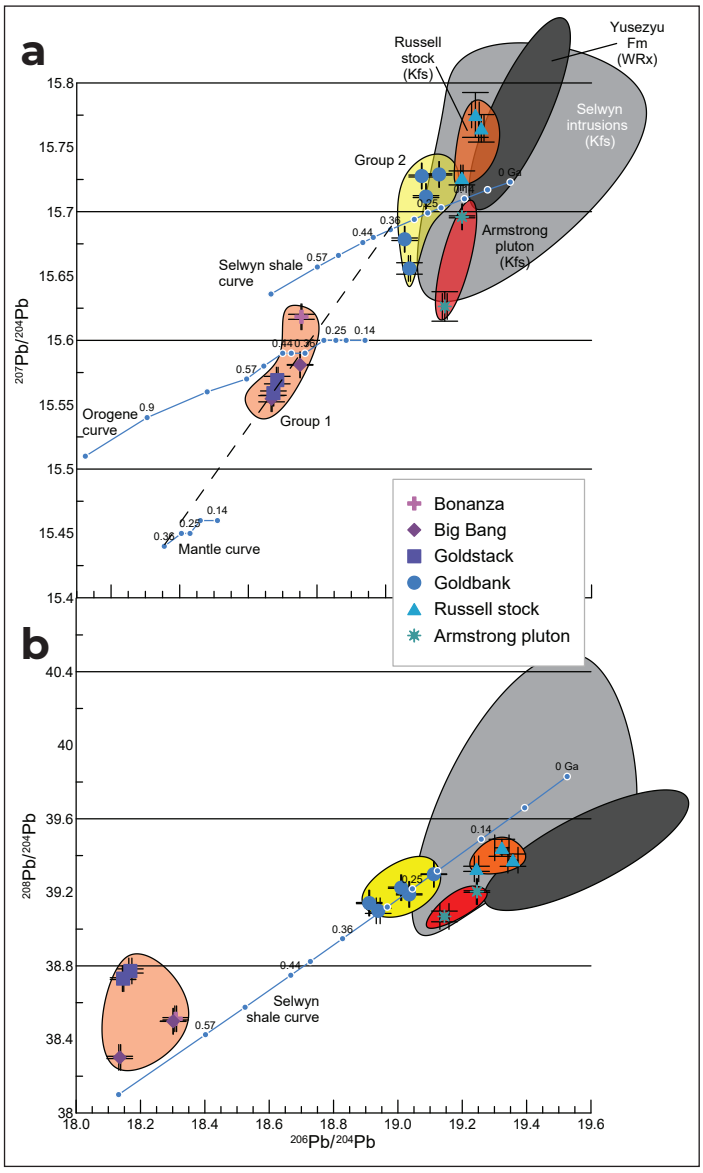

Figure 14. *Plot of* ***(a)*** *Uranogenic lead and* ***(b)*** *Thorogenic lead for galena and feldspar from the Plateau area. Included are previously published feldspar data from 'Selwyn basin area' plutons compiled in Rasmussen (2013) and whole-rock Pb isotope analyses from the Yusezyu Formation courtesy of Ben Cave (written communication, 2018). Mantle and orogene curves are from Zartman and Doe (1981) and the Selwyn shale curve is from Godwin and Sinclair (1982). Dashed line ties ca. 360 Ma mantle, orogene and Selwyn shale curves together.*

2. All mineralization relates to Early Cretaceous (*ca.* 130 to 100 Ma) orogenic fluids. In this interpretation, the younger muscovite and sericite ages in the Goldbank area are a result of thermal resetting by intrusions and the bimodal nature of Pb isotopic data is the result of local (<10 km?) metal sources. Primitive lead could have come from mafic rocks such as those mapped on the western portion of the property (Stubley, 2017) and the more isotopically evolved Pb would reflect hydrothermal circulation in country rocks without a primitive component.

Discussion and further work

This is an initial attempt to constrain the origin of gold mineralization in the Plateau area. We present evidence for orogenic gold mineralization but consider the identification of intrusion-related gold mineralization subjective. Better understanding of the age of regional metamorphism and mineralization would boost confidence in the interpretation of mineralization associated with both regional metamorphism and pluton emplacement. For example, *in situ* muscovite dating may constrain the age of individual ductile deformation events in the area, breaking mineralization into discrete events as opposed to our current suggestion of a single protracted event. Similarly, if additional Pb isotope data with well-constrained paragenesis could be petrographically linked to deformation or intrusive events, a stronger interpretation on the importance of intrusion-related mineralization would be possible.

References

Allan, M., Rhys, D.A. and Hart, C.J.R., 2017. Orogenic gold mineralization of the eastern Cordilleran gold belt, British Columbia: Structural ore controls in the Cariboo (093A/H), Cassiar (104P) and Sheep Creek (082F) mining districts. Geoscience BC, Report 2017-15, 108 p.

Barr, T., 2017. Fluid inclusion analysis of the Plateau Gold project, Yukon, Canada. BSc thesis, University of Alberta, 27 p.

Cecile, M.P., 2000. Geology of the northeastern Niddery Lake map area, east-central Yukon and adjacent Northwest Territories. Geological Survey of Canada, Bulletin 553, 128 p.

Colpron, M. and Nelson, J.L., 2011. A digital atlas of terranes for the northern Cordillera. Yukon Geological Survey, also, BC Geological Survey, GeoFile 2011-11.

Dubé, B. and Gosselin, P., 2007. Greenstone-hosted quartz-carbonate vein deposits *In*: Mineral Deposits of Canada: A Synthesis of Major Deposit-types, District Metallogeny, the Evolution of Geological Provinces, and Exploration Methods, W.D. Goodfellow (ed.), Special Publication 5, Mineral Deposits Division, Geological Association of Canada, p. 49–73.

Farquharson, J., 2017. A microstructural analysis of Goldstrike's Plateau property, Yukon. BSc thesis, Lakehead University, 67 p.

Frost, B.R., Barnes, C.G., Collins, W.J., Arculus, R.J., Ellis, D.J. and Frost, C.D., 2001. A geochemical classification for granitic rocks. Journal of Petrology, vol. 42, no. 11, p. 2033–2048.

Godwin, C.I. and Sinclair, A.J., 1982. Average lead isotope growth curves for shale-hosted zinc-lead deposits, Canadian Cordillera. Economic Geology, vol. 77, no. 3, p. 675–690.

Goldfarb, R.J., Baker, T., Dube, B., Groves, D.I., Hart, C.J.R. and Patrice, G., 2005. Distribution, character, and genesis of gold deposits in metamorphic terranes *In*: Economic Geology: One Hundredth Anniversary Volume, J.W. Hedenquist, J.F.H. Thompson, R.J. Goldfarb and J.P. Richards (eds.), Society of Economic Geologists, p. 407–450.

Hart, C.J.R., Mair, J.L., Goldfarb, R.J. and Groves, D.I., 2004. Source and redox controls on the metallogenic variations in intrusion-related ore systems, Tombstone-Tungsten Belt, Yukon Territory, Canada. Transactions of the Royal Society of Edinburgh: Earth Sciences, vol. 95, p. 339–356.

Heffernan, S. and Mortensen, J.K., 2000. Age, geochemical and metallogenic investigations of Cretaceous intrusions in southeastern Yukon and southwestern NWT: A preliminary report *In*: Yukon Exploration and Geology 1999, D.S. Emond and L.H. Weston (eds.), Exploration and Geological Services Division, Yukon, Indian and Northern Affairs Canada, p. 145–149.

Mair, J.L., Hart, C.J.R. and Stephens, J.R., 2006. Deformation history of the northwestern Selwyn Basin, Yukon, Canada: Implications for orogen evolution and mid-Cretaceous magmatism. Geological Society of America Bulletin, vol. 118, no. 3/4, p. 304–323.

Maniar, P.D. and Picolli, P.M., 1989. Tectonic discrimination of granitoids. Geological Society of America Bulletin, vol. 101, no. 5, p. 635–643.

Mortensen, J.K. and Gabites, J.E., 2002. Lead isotopic constraints on the metallogeny of southern Wolf Lake, southeastern Teslin and northern Jennings River map areas, Yukon and British Columbia: Preliminary results *In*: Yukon Exploration and Geology 2001, D.S. Emond, L.H. Weston and L.L. Lewis (eds.), Exploration and Geological Services Division, Yukon Region, Indian and Northern Affairs Canada, p. 179–188.

Murphy, D., 1997. Geology of the McQuesten River region, northern McQuesten and Mayo map areas, Yukon Territory (115P/14, 15, 16; 105M/13, 14). Indian and Northern Affairs Canada, Exploration and Geological Services Division, Yukon, Bulletin 6, 122 p.

Pigage, L.C., 2004. Bedrock geology compilation of the Anvil district (parts of NTS 105K/2, 3, 5, 6, 7 and 11), central Yukon. Yukon Geological Survey, Bulletin 15, 103 p.

Rasmussen, K.L., 2013. The timing, composition and petrogenesis of syn- to post-accretionary magmatism in the northern Cordilleran miogeocline, eastern Yukon and southwest Northwest Territories. PhD thesis, University of British Columbia, 810 p.

Richards, J.P., 2015. Petrographic and paragenetic relationships of seventeen samples from the Goldstack and Gold Dome zones, Plateau Gold deposit, Yukon. Internal company report.

Roach, S., 2013. Report of 2012 surface exploration and diamond drill program on the Plateau South project. Yukon Energy, Mines and Resources Assessment Report AR096441.

Roots, C.F., 1998. Progress report on bedrock geology of Lansing map area, central Yukon Territory. Geological Survey of Canada, Current Research 1998-A, p. 19–28.

Roots, C.F., 2003. Bedrock geology of Lansing Range map area (NTS 105N), central Yukon (scale). Yukon Geological Survey and Geological Survey of Canada, Geoscience Map 2003-1, scale 1:250 000.

Roots, C.F., Abbott, J.G., Cecile, M.P., Gordey, S.P. and Orchard, M.J., 1995. New stratigraphy and structures in eastern Lansing map area, central Yukon Territory. Geological Survey of Canada, Current Research 1995-A, p. 141–147.

Sack, P.J., Kruse, S. and Ferraro, D., 2018. Gold occurrences on the Plateau South property (Yukon MINFILE 105N 034, 035, 036), central Yukon. *In*: Yukon Exploration and Geology Overview 2017, K.E. MacFarlane (Ed.), Yukon Geological Survey, p. 75–91.

Staples, R.D., Murphy, D.C., Gibson, H.D., Colpron, M., Berman, R.G. and Ryan, J.J., 2014. Middle Jurassic to earliest Cretaceous mid-crustal tectono-metamorphism in the northern Canadian Cordillera: Recording foreland-directed migration of an orogenic front. Geological Society of America Bulletin, vol. 126, no. 11-12, p. 1511–1530.

Stubley, M., 2017. Structural architecture of the Plateau property: Some preliminary comments (NTS 105N). Internal company report.

Tosdal, R.M., Wooden, J.L. and Bouse, R.M., 1999. Pb isotopes, ore deposits, and metallogenic terranes *In*: Reviews in Economic Geology, Volume 12, D.D. Lambert and J. Ruiz (eds.), Society of Economic Geology, p. 1–28.

Vanwermeskerken, M., 2017. Detailed geologic mapping at Goldstack, Goldstack Lake and Bonanza zones *In*: 2016 diamond drilling, geological mapping and structural analysis on the Plateau Property, D. Ferraro, Yukon Energy, Mines and Resources Assessment Report 097024.

Yukon Geological Survey, 2018a. Yukon MINFILE - A database of mineral occurrences, https://data.geology.gov.yk.ca, [accessed April 23, 2018].

Yukon Geological Survey, 2018b. Yukon Digital Bedrock Geology, http://data.geology.gov.yk.ca/Compilation/3, [accessed April 25, 2018].

Zartman, R.E. and Doe, B.R., 1981. Plumbotectonics–The model. Tectonophysics, vol. 75, p. 135–162.

Appendices

The appendices are only available as digital files. They are included in a .zip file that accompanies this document, and are available from https://data.geology.gov.yk.ca.

Appendix 1. Plateau geochemistry and QEMSCAN.

Appendix 2. U-Pb geochronology.

Appendix 3. Ar geochronology.